

Synthesis of Wall-thickness-controllable BiFeO₃ Nanotubes by Sol–Gel Method

Wenfeng Xiang,¹ Rui Sun,¹ Chenghao Hu,² Jiangfeng Yao,¹
Zibin Dong,¹ Shaohua Chen,^{1*} and Haizhong Guo^{3**}

¹Beijing Key Laboratory of Optical Detection Technology for Oil and Gas, China University of Petroleum,
18 Fuxue Road, Changping District, Beijing 102249, China

²Department of Physics, University of Science and Technology Beijing,
30 Xueyuan Road, Haidian District, Beijing 100083, China

³School of Physical Engineering, Zhengzhou University,
100 Kexuedadao Road, Zhongyuan District, Zhengzhou, Henan 450001, China

(Received December 18, 2017; accepted May 5, 2018)

Keywords: BiFeO₃ nanotubes, controllable thickness, pump speed

Wall-thickness-controllable multiferroic bismuth ferrite (BiFeO₃) nanotubes were synthesized by a sol–gel method combined with an anodic aluminum oxide (AAO) template. By connecting the template with a negative pressure system tuned by a gas flowmeter, BiFeO₃ nanotubes with wall thicknesses of about 28 and 15 nm were obtained if the flowmeter speed was adjusted to 0.4 and 2 m³/h, respectively. The resulting nanotubes were characterized by energy dispersive spectroscopy (EDS), X-ray diffraction (XRD), and scanning electron microscopy (SEM) techniques. It is shown that the nanotubes present a rhombohedral distorted perovskite BiFeO₃ structure. Meanwhile, the wall thickness of BiFeO₃ nanotubes became smaller at higher flowmeter speed, which was caused by the increase in the differential pressure on the solution.

1. Introduction

Single-phase multiferroics, defined as materials presenting at least two ferric properties within a single phase, have attracted extensive attention owing to their fascinating physical properties and potential applications in technologies involving data storage, memories, and sensor devices.^(1–3) However, the number of single-phase multiferroics is not very high. Owing to its high Curie temperature ($T_c = 1103$ K), high Neel temperature ($T_N = 643$ K), and large residual polarization intensity (150 $\mu\text{C}/\text{cm}^2$), BiFeO₃ is considered as one of the few known single-phase multiferroic materials at room temperature.^(4,5) However, a weak linear magnetoelectric coupling makes it difficult to be applied to multifunctional storage devices.⁽⁶⁾ Fortunately, BiFeO₃ nanostructures of below 62 nm size are predicted to present a relatively strong ferromagnetism, which means that the linear magnetoelectric coupling⁽⁷⁾ will increase in

*Corresponding author: e-mail: shchen@cup.edu.cn

**Corresponding author: e-mail: hguo@zzu.edu.cn

<http://dx.doi.org/10.18494/SAM.2018.1855>

the nanostructure. Consequently, many studies on the BiFeO₃ nanodevice have been carried out in recent years.^(6–8)

Compared with zero- and two-dimensional structures, the synthesis of a one-dimensional nanostructure is highly significant, because its special properties are strongly dependent on dimension and size. However, research progress is very slow. Take BiFeO₃ nanotubes as an example. Up to now, they have been successfully fabricated by various approaches, such as by electrostatic spinning, template, sol–gel, and hydrothermal methods.^(8–14) However, there are few reports on their controllable fabrication, which is necessary for studying size-dependent physical properties related to potential applications to engineering devices.

In this work, a simple and controllable sol–gel wetting anodic aluminum oxide (AAO) template approach was designed to synthesize BiFeO₃ nanowires with different wall thicknesses. The template was set onto a negative pressure system tuned by a gas flowmeter. By changing the speed of the gas flowmeter, the negative pressure on the solution, as well as the wall thickness of the nanotubes, could be controlled. The as-prepared BiFeO₃ nanotubes were characterized by energy dispersive spectroscopy (EDS), X-ray diffraction (XRD), and scanning electron microscopy (SEM) techniques, and the thickness control principle was also analyzed.

2. Fabrication Process

2.1 Chemical synthesis

BiFeO₃ nanowires were fabricated by an AAO template-based sol–gel method, where the solution was synthesized by a chemical route.⁽¹⁰⁾ Bismuth nitrate (BiNO₃·5H₂O) and iron nitrate (FeNO₃·9H₂O) with a molar ratio of 1:1 were dissolved in 2-methoxyethanol (C₃H₈O₂) and stirred for 30 min at room temperature. By adding 2-methoxyethanol and nitric acid, the solution concentration and pH value were adjusted to 0.3 M and 4–5, respectively, and the ferrioxalate precursor was obtained. Subsequently, the precursor was dropped onto the AAO membrane (Whatman Anodisc®).

After being deposited onto the AAO membrane, the precursor would wet the template. Unfortunately, the pore diameter was only about 150 nm, so that it was difficult for a viscous precursor to fill the template. Consequently, a negative pressure system was selected to facilitate the precursor flow along the template pore; the schematic diagram is shown in Fig. 1. It could be seen that the system is composed of the common negative pressure system in the

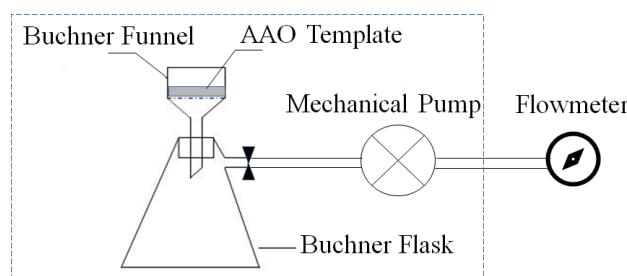


Fig. 1. Schematic structure of flowmeter controlling negative pressure system and AAO template.

frame and a gas flowmeter, which is specially utilized to quantitatively tune the mechanical pump velocity.

After being filled by the BiFeO₃ precursor, the AAO template was preheated in a drying oven at 100 °C for 1 h, and annealed in air ambient at 750 °C for 2 h. To remove the template and release the BiFeO₃ nanotubes, the template was immersed in 4 M NaOH solution for 6 h at room temperature. Thereafter, the base liquid was cleaned in several steps with deionized water, and the solution containing only nanotubes and deionized water could be obtained.

2.2 Characterization methods

Analysis of the component and crystallinity of the samples was carried out by EDS and XRD with Cu- $\kappa\alpha$ radiation. The morphology of BiFeO₃ nanotubes was characterized by SEM (SEM, FEI Quanta 200F Sirion FEG) with acceleration voltages of 200 V–30 kV.

3. Results and Discussion

Figure 2 shows the SEM image of free nanotubes after the template is etched off. It is shown that the nanotubes longer than 10 μm have been successfully fabricated. The EDS image of the as-prepared nanotubes is shown in Fig. 3. The expected element peaks from Bi, Fe, and O are presented, where the atomic ratio of the elements Bi and Fe is about 1:1, indicating that the nanotubes are composed of the BiFeO₃ phase. Meanwhile, there are some other elements, namely, Na, Al, and Si that remain in the NaOH solution, AAO template, and silicon plate holding the solution, respectively. Figure 4 shows the XRD spectra of the nanotubes. It is shown that most peaks can be identified as BiFeO₃ with a rhombohedrally distorted perovskite structure, and the unindexed peaks possibly originated from the impurities, including the remaining AAO template, NaOH, and silicon plate.

SEM images showing the morphologies of BiFeO₃ nanotubes are shown in Figs. 5(a) and 5(b), with pump velocities of 0.4 and 2 m^3/h , respectively. For the 0.4 m^3/h velocity, the

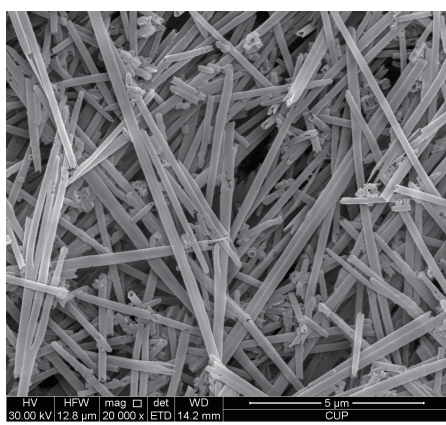


Fig. 2. Top-view SEM image of the AAO template containing the BFO precursors.

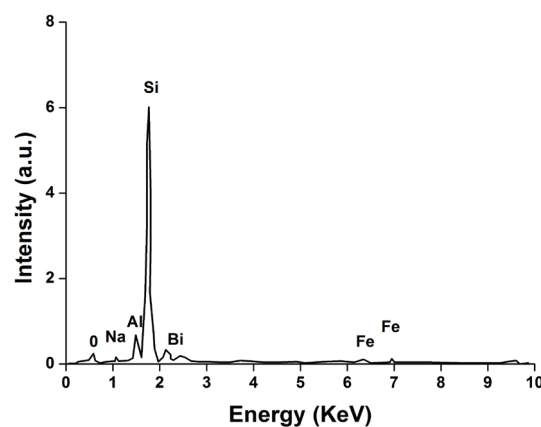


Fig. 3. EDS images of BFO nanotubes.

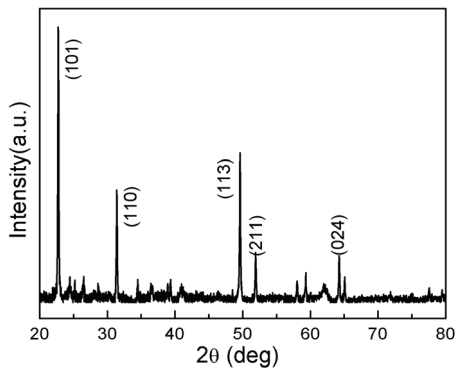
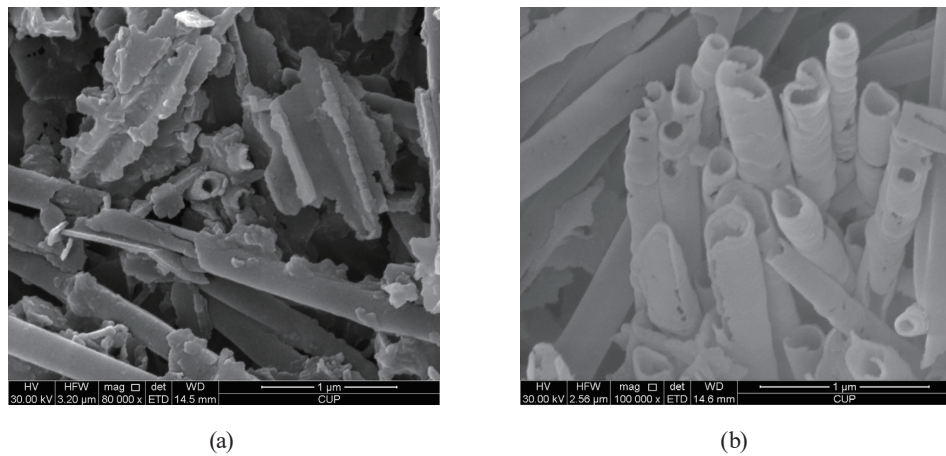


Fig. 4. XRD images of BFO nanotubes.

Fig. 5. SEM images of BFO nanotubes fabricated with different flowmeter speeds of (a) 0.4 and (b) 2 m³/h.

nanotubes are smooth and complete, with the wall thickness ranging from 25 to 29 nm. For the 2 m³/h velocity, the nanotubes have wall thicknesses ranging from 14 to 15 nm. At the same time, some holes or other types of defects appear in the nanotubes. Additionally, it is discovered in the experiment that the length of the nanotubes is shorter than that for the 0.4 m³/h velocity.

By comparing Fig. 5(a) with Fig. 5(b), it could be seen that the morphology of the nanotubes is affected by the pump velocity. The wall becomes thinner and weaker with a higher speed, which can be explained as follows. Under normal air pressure conditions, the solution would infiltrate into and attach to the pore wall mainly by the capillary effect. However, owing to the high viscosity of the solution and upward pressure from the remaining atmosphere in the pore, it is very difficult for the solution to enter the narrow pore. When the mechanical pump works, the air density and pressure of the Buchner flask in Fig. 1 would decrease to less than those under normal air pressure on top of the solution. The downward differential pressure could drive the air out of the pore, which is beneficial for solution flow throughout the pore. During the flowing process, it could wet and fill the entire pore at the beginning, and then the central part would be drawn out of the pore by the differential pressure, which leads to the nanotubes

coming into being after annealing. When the pump works at a higher speed, less solution would be left in the pore and the nanotube wall would become thinner. However, if it is too high, some defects such as holes or cracks would appear in the weak portion of the nanotube after annealing, which means that the performance of the nanotubes is becoming worse. Clearly, the mechanical pump should work below that velocity.

4. Conclusions

For the first time, thickness-controllable BiFeO₃ nanotube arrays have been successfully synthesized using sol-gel wetting AAO templates assisted by a negative pressure system. The gas flowmeter is applied to quantitatively tune the velocity of the mechanical pump, and the nanotube thickness could be continuously controlled. EDS and XRD investigations illustrate that the nanotubes with different thicknesses are composed of the same perovskite BiFeO₃ structure. It is considered that the tunable negative pressure system would have wide prospects for thickness-controllable nanotube fabrications.

Acknowledgments

This work was supported by the National Natural Science Foundation of China (Grant Nos. 11774026 and 11004251) and Excellent Young Teachers Program of the China University of Petroleum (2462015YQ0603).

References

- 1 S. Farokhipoor, C. Magen, S. Venkatesan, J. Iniguez, C. J. M. Daumont, D. Rubi, E. Snoeck, M. Mostovoy, C. de Graaf, A. Müller, M. Doblinger, C. Scheu, and B. Noheda: *Nature* **515** (2014) 379.
- 2 K. Chu, B. K. Jang, J. H. Sung, Y. A. Shin, E. S. Lee, K. Song, J. H. Lee, C. S. Woo, S. J. Kim, S. Y. Choi, T. Y. Koo, Y. H. Kim, S. H. Oh, M. H. Jo, and C. H. Yang: *Nat. Nanotechnol.* **10** (2015) 972.
- 3 Q. Q. Yang, H. Zhang, K. H. Linghu, X. G. Chen, J. B. Zhang, R. J. Nie, F. R. Wang, J. X. Deng, and J. Y. Wang: *J. Alloys Compd.* **646** (2015) 1133.
- 4 T. E. Quickel, L. T. Schelhas, R. A. Farrell, N. Petkov, V. H. Le, and S. H. Tolbert: *Nat. Commun.* **6** (2015) 6562.
- 5 Z. X. Li, Y. Shen, Y. H. Guan, Y. H. Hu, Y. H. Lin, and C. W. Nan: *J. Mater. Chem. A* **2** (2014) 1967.
- 6 T. Zhao, A. Scholl, F. Zavaliche, K. Lee, M. Barry, A. Doran, M. P. Cruz, Y. H. Chu, C. Ederer, N. A. Spaldin, R. R. Das, D. M. Kim, S. H. Baek, C. B. Eom, and R. Ramesh: *Nat. Mater.* **5** (2006) 823.
- 7 T. Park, G. C. Papaefthymiou, A. J. Viescas, A. R. Moodenbaugh, and S. S. Wong: *Nano Lett.* **7** (2007) 766.
- 8 T. J. Park, Y. Mao, and S. S. Wong: *Chem. Commun.* **23** (2004) 2708.
- 9 X. Y. Zhang, J. Y. Dai, and C. W. Lai: *Prog. Solid State Chem.* **33** (2005) 147.
- 10 F. Gao, Y. Yuan, K. F. Wang, X. Y. Chen, F. Chen, and J. M. Liu: *Appl. Phys. Lett.* **89** (2006) 102506.
- 11 B. Liu, B. B. Hu, and Z. L. Du: *Chem. Commun.* **47** (2011) 8166.
- 12 Y. Zhao, J. Miao, X. S. Zhang, and Y. Z. Jiang: *J. Mater. Sci. - Mater. Electron.* **23** (2012) 180.
- 13 K. Prashanthi, P. M. Shaibani, A. Sohrabi, T. S. Natarajan, and T. Thundat: *Phys. Status Solidi RRL* **6** (2012) 244.
- 14 L. A. S. de Oliveira and K. R. Pirota: *J. Sol-Gel Sci. Technol.* **63** (2012) 275.